Metabolic Consequences of Phosphotransferase (PTS) Mutation in a Phenylalanine-Producing Recombinant Escherichia coli

ARTICLE *in* BIOTECHNOLOGY PROGRESS · DECEMBER 1997

Impact Factor: 2.15 · DOI: 10.1021/bp970060h · Source: OAI

Metabolic Consequences of Phosphotransferase (PTS) Mutation in a Phenylalanine-Producing Recombinant *Escherichia coli*

Ruizhen Chen,[†] Vassily Hatzimanikatis,[‡] Wyanda M. G. J. Yap,[§] Pieter W. Postma,[§] and James E. Bailey*[,‡]

Department of Chemical Engineering, California Institute of Technology, Pasadena, California 91125

E. coli strain PPA305, which has a wild-type PTS system, and PPA316, which utilizes a proton-galactose symport system for glucose uptake, were used as host strains to harbor a phenylalanine overproduction plasmid pSY130-14 and to study the effects of using different glucose uptake systems on phenylalanine production. The non-PTS strain (PPA316/pSY130-14) produced much less phenylalanine, ranging from 0 to 67% of that produced by the PTS strain (PPA305/pSY130-14) depending on cultivation conditions used. The non-PTS strain PPA316/pSY130-14 had an intracellular PEP concentration only one-sixth that of the PTS strain, PPA305/pSY130−14. Additionally, PPA316/pSY130-14 had a substantially lower energy state in terms of the size of the pool of high-energy phosphate compounds and the magnitude of the pH difference across the cytoplasmic membrane. The non-PTS strain consumed oxygen at a higher rate, attained lower biomass concentration, and produced no acetate and phenylalanine during fermentation, suggesting more carbon was oxidized to CO_2, most likely through the TCA cycle. Analysis of intracellular fluxes through the central carbon pathways was performed for each strain utilizing exponential phase data on extracellular components and assuming quasi-steady state for intermediate metabolites. The non-PTS strain had a higher flux through pyruvate kinase (PYK) and TCA cycle which, in agreement with the observed higher oxygen uptake rate, suggests that more carbon was oxidized to CO_2 through the TCA cycle. Further analysis using rate expression data for PYK and NMR data for the intracellular metabolites identified the regulatory properties of PYK as the probable cause for lower intracellular PEP levels in PPA316/pSY130-14.

Introduction

Plants and microbes are known to possess abilities to convert simple carbohydrates such as glucose to aromatic amino acids and related metabolites (Weiss and Edwards, 1980). The aromatic amino acids phenylalanine, tyrosine, and tryptophan produced industrially are mainly used as human and animal dietary supplements. Microbial production of other compounds derived from these three aromatic amino acids such as the important dye indigo and eumelanin, which has unique UV-absorbing characteristics (Draths *et al.*, 1992; Bell and Wheeler, 1986), are being pursued for specific applications. The production of phenylalanine is of particular interest because it is one of the essential raw materials in the manufacture of the low-calorie sweetener aspartame, which is estimated to be at least 150 times sweeter than sucrose (Huang *et al.*, 1985) and presently enjoys a large market worldwide.

Phenylalanine is synthesized from its precursors phosphoenolpyruvate (PEP) and erythrose 4-phosphate (E4P) through a highly controlled biosynthesis pathway. Figure 1 presents a simplified representation of the phenylalanine biosynthesis pathway of *E. coli*, showing the involvement of all major precursors, reducing equivalents and ATP. Also indicated in Figure 1 are two regulatory enzymes whose controls are affected by a combination of feedback inhibition, feedback repression, and attenuation (Pittard, 1987). DAHP synthase, which catalyzes the first committed step in the pathway, the condensation of PEP and E4P to synthesize 3-deoxyarabinoheptulosonate 7-phosphate (DAHP), serves as the first control. *E. coli* has three isoenzymes of DAHP synthase, each subject to feedback control at both genetic and enzymatic levels by a different amino acid (AroG by phenylalanine, AroF by tyrosine, and AroH by tryptophan). The other

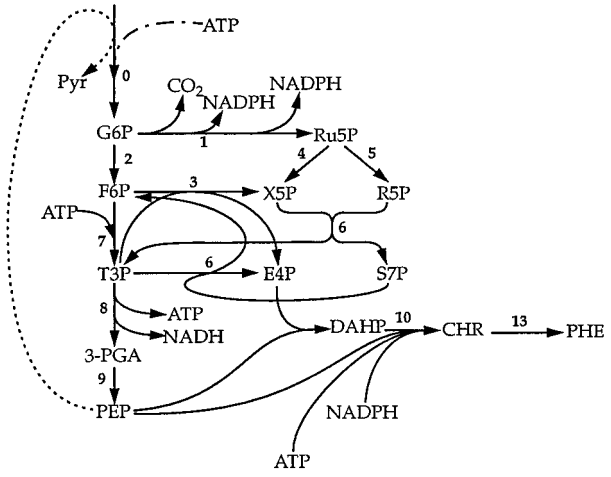

Figure 1. Phenylalanine synthesis pathway considered for estimates of the maximum theoretical yields for phenylalanine and ATP.

[†] Current address: Fermentation Development Laboratory, Bristol-Myers Squibb Co., Syracuse, NY 13221.

[‡] Institute of Biotechnology, ETH-Zurich, CH-8093 Zurich, Switzerland.

[§] E.C. Slater Institute, Plantage Muidergracht 12, 1018 TV Amsterdam, The Netherlands.

* Corresponding author.

S8756-7938(97)00060-X CCC: $14.00

regulatory enzyme is a bifunctional enzyme, chorismate mutase P-prephenate dehydratase, catalyzing two reactions from chorismate to phenylpyruvate (Figure 1). Synthesis of chorismate mutase P-prephenate dehydratase is repressed by phenylalanine and is also regulated at the level of transcriptional termination by attenuation (Brown, 1968; Zurawski *et al.*, 1978). Phenylalanine also inhibits the activity of this enzyme. Because of rigorous regulation of the pathway by the end product, only genetically modified strains will produce phenylalanine in quantities substantially greater than that required for cell growth.

Metabolic engineering has been successfully applied previously to deregulate the phenylalanine biosynthetic pathway. Genetic strain improvement has been facilitated by detailed knowledge of the biosynthetic pathway and its regulation. Regulation at the genetic level can be circumvented by replacing native promoters with strong heterologous promoters so that the expression of the enzymes involved in the phenylalanine production is controlled by an added chemical (e.g., IPTG), by temperature, or by other means (Sugimoto *et al.*, 1987). Selecting resistance to a toxic phenylalanine analogue has been used to isolate rapidly mutants with biosynthetic enzymes which are not feedback inhibited by phenylalanine (Backman *et al.*, 1990; Sugimoto *et al.*, 1985). Using these methods, a hyperproducing *E. coli* strain can be constructed which, in concert with a well-matched fermentation process (Backman *et al.*, 1990; Konstantinov, 1991), can attain a final phenylalanine concentration of 50 g/L.

Wild-type *E. coli* use a phosphotransferase system (PTS) for glucose uptake. The main feature of the PTS system which is pertinent here is its catalysis of glucose phosphorylation using PEP as the phosphate donor and producing pyruvate, along with glucose 6-phosphate, as products (for a recent review of the PT system, see Postma *et al.*, 1993). In the normal case in which pyruvate is not converted back to PEP, this reaction leaves only three carbons of the entering six per glucose available for aromatic amino acid biosynthesis from PEP. Therefore, the theoretical yield of phenylalanine based on glucose can be doubled (see, for example, Forberg *et al.* (1988), Forberg and Haggstrom (1988), and below) by modifying the production organism to use a different glucose uptake system which does not use PEP as a phosphate donor. Prior research has identified *E. coli* mutants with an inactivated PTS uptake system as well as mutations which make the normally inducible proton−galactose symport system constitutive, the combination of which switches glucose uptake to the proton−galactose symport system and glucose phosphorylation to the ATP-dependent glucokinase (Postma, 1987). (Alternatively, the cells can be engineered to overexpress PEP synthase to recycle pyruvate to PEP; see Patnaik and Liao (1994).) In this work, contemporary genetic methods have been used to construct two otherwise isogenic *E. coli* strains, one using PTS and the other galatose symport (GalP) glucose uptake, so that the metabolic characteristics of these two alternative systems can be systematically investigated.

Bioreactor cultivations were conducted to compare specific growth rates, phenylalanine accumulation, and byproduct production in two *E. coli* strains, one engineered to use only PTS glucose uptake and the other engineered to employ only the galactose−proton symport system for glucose uptake. Both strains were transformed with a plasmid containing several genes which confer a phenylalanine overproduction phenotype (Sugimoto *et al.*, 1987). Using these data, intracellular fluxes were estimated by metabolic flux analysis based on known pathway stoichiometry. This information was enhanced by additional measurements using phosphorous-31 nuclear magnetic resonance spectroscopy (^{31}P NMR). In particular, ^{31}P NMR was employed to monitor *in vivo* the following cell energetic and composition parameters: ΔpH across the cytoplasmic membrane and NTP, NAD(H) and total sugar phosphate (SP) concentrations (Chen and Bailey, 1993, 1994). Intracellular concentrations of intracellular sugar phosphates were determined by ^{31}P NMR analysis of perchloric acid (PCA) extracts.

Materials and Methods

Strains and Plasmid. *E. coli* K-12 strain MG1655 was obtained from Carol Gross. PPA305 (*galP::*Tn10) was constructed via P1 transduction using *E. coli* UE7 (*thi* Δ(*ptsH1-crr*) *galR galP::*Tn*10*) (Boos *et al.*, 1987) as donor and MG1655 as recipient. PPA309 (Δ(*ptsH1-crr*)-*zfc-706::*Tn*10*) was derived from MG1655 by P1 transduction with a lysate of *E. coli* UE1 (*thi* Δ(*ptsH1-crr*) *zfc-706::*Tn*10 galR*) (W. Boos, University of Konstanz, Germany). Strain PPA316 (Δ(*ptsH1-crr*) *zfc-706::*Tn*10 galR*) was isolated from PPA309 by selecting for growth on glucose minimal plates.

Plasmid pSY130-14 (Sugimoto *et al.*, 1987) was kindly provided by Dr. T. Yoshida (Osaka University, Japan). pSY130-14 carries the genes *aro*F^{FR} and *phe*A^{FR} for the enzymes involved in the critical regulated steps in the phenylalanine synthesis pathway. The mutated gene *aroF*^{FR}, which encodes 3-deoxy-D-arabino-heptulosonate 7-phosphate synthase catalyzing the condensation of erythrose-4-P and PEP, is resistant to feedback inhibition by tyrosine. The mutated gene *pheA*^{FR}, which encodes chorismate mutase P-prephenate dehydratase catalyzing the formation of prephenate from chorismate, is resistant to feedback inhibition by phenylalanine. Expression of *aroF*^{FR} and *pheA*^{FR} are controlled by a P_R-P_L promoter and temperature-sensitive repressor cI_{857} of bacteriophage λ. In the host and process used in the original study (Sugimoto *et al.*, 1987), the optimal temperature for phenylalanine production was found to be 38.5 °C.

Medium and Culture Conditions. The medium used in this study contained (per liter): glucose, 20 g; $Na_2HPO_4 \cdot 7H_2O$, 12.8 g; KH_2PO_4, 3 g; NaCl, 1 g; NH_4Cl, 2 g; $MgSO_4 \cdot 7H_2O$, 3 g; sodium glutamate, 0.4 g; $CaCl_2$, 11 mg; $FeSO_4 \cdot 7H_2O$, 10.7 mg; $ZnCl_2 \cdot 7H_2O$, 0.8 mg; $MnSO_4$, 8 mg; $CuSO_4 \cdot 5H_2O$, 10.7 mg; $(NH_4)_6Mo_7O_{24} \cdot 4H_2O$, 6.7 mg; $Co(NO_3)_2$, 6.7 mg. Antifoam poly(propylene glycol) (1.0 mL/L) (MW 1000) was added. Kanamycin (12.5 mg/L) was used for selection of plasmid-containing strains.

Fermentations were performed aerobically in a 3.5 L (working volume 1.5 L) LH bioreactor (LH Fermentation, Hayward, CA). pH was controlled at 7.0 by automatic addition of 30% NH_4OH. Air flow rate was fixed at 2.0 L/min; dissolved oxygen was maintained above 20% of air saturation by manually adjusting agitation speed for the PTS strain or by oxygen enrichment to the air for the non-PTS strain (the non-PTS strain has a much higher specific oxygen uptake rate than the PTS strain which makes oxygen enrichment necessary to maintain the same DO level in the bioreactor, see also Discussion). All fermentations were conducted at 38.5 °C. The inocula were prepared with LB supplemented with kanamycin and grown overnight at 30 °C in a shaker. Inoculation (2% v/v) was used in all fermentations.

In shake-flask cultivation, cells were grown using 500 mL flasks containing 50 mL of the medium described above. The cultivation was carried out at 275 rpm in an

INNOVA 4000 rotary shaker (New Brunswick Scientific) and at either a uniform temperature 38.5 or at 30 °C followed by a shift to 38.5 °C.

Analytical Methods. Dry weight cell concentration in cell suspension samples taken from the fermentor was measured as follows: After two washes, the cell pellet was transferred to a preweighed aluminum plate which was dried at 105 °C to constant weight. Metabolites in the supernatants were analyzed by high-performance liquid chromatography (HPLC). A Bio-Rad Aminex HXP-87H (300 × 7.8 mm) column was used, and a 0.01 N H_2PO_4 mobile phase at flow rate 0.4 mL/min was found to be satisfactory in resolving metabolites of interest (Diaz-Ricci *et al.*, 1990). Glucose concentration in the medium was determined with a Sigma test kit (510-A). Ethanol and D-lactate were assayed using Boehringer-Mannheim kits. All absorbance measurements were made using a Shimadzu UV-260 spectrophotometer. Phenylalanine was measured using a Sigma kit F-60 on a Shimadzu spectrofluorophotometer at an emission wavelength of 480 nm and excitation wavelength of 390 nm.

NMR Experiments. *E. coli* cells were grown at 38.5 °C and 275 rpm in a rotary shaker (New Brunswick Scientific) in 2 L shake flasks in 1 L of the same medium as detailed above. All subsequent sample preparation procedures and NMR operations were as described elsewhere (Chen *et al.*, 1996).

Results

Analysis of Metabolic Stoichiometry. Before examining experimental data, it is useful to analyze the effects of changing from PTS to galactose symport glucose uptake on the theoretical energy and phenylalanine yields. Such an analysis has been undertaken, considering the metabolic reaction network for phenylalanine production in *E. coli* shown in Figure 1. The results of this stoichiometric analysis depend strongly on the assumptions made concerning utilization of reduced pyridine nucleotide cofactors. As case 1, we assume that transhydrogenase activity is absent (that is, interconversion of NADH and NADPH does not occur) and that all NADPH produced by the pentose phosphate cycle is used for phenylalanine biosynthesis. In this case, the following overall stoichiometric relationships for the metabolic network can be be derived:

for PTS uptake (case 1):

$$21\ \text{glucose} + 9\text{ADP} + 9\text{P}_\text{i} + 6\text{NH}_3 + 33\ \text{NAD}^+ \rightarrow 6\ \text{phenylalanine} + 21\ \text{pyruvate} + 9\text{ATP} + 9\text{CO}_2 + 33\text{NADH} + 33\text{H}^+$$

for galactose symport uptake (case 1):

$$21\ \text{glucose} + 24\text{ATP} + 12\ \text{NH}_3 + 24\ \text{NAD}^+ \rightarrow 12\ \text{phenylalanine} + 24\text{ADP} + 24\text{P}_\text{i} + 18\text{CO}_2 + 24\text{NADH} + 24\text{H}^+$$

These stoichiometries indicate that twice as much phenylalanine can be made using GalP glucose uptake compared to PTS uptake. However, this benefit is associated with a significant deterioration of energy yield in the GalP case. This system must hydrolyze a substantial amount of ATP, while the PTS organism generates net ATP from these pathways. The ATP deficit in the GalP system can of course be addressed by considering in addition oxidation of NADH via the respiratory chain. However, the PTS strain has even more NADH available and, therefore, retains superior energy yield if respiration is considered.

As an alternative scenario, stoichiometric analysis has been conducted of a different situation, designated case 2, in which we assume that transhydrogenase is present and that any reduced pyridine nucleotides produced which are not used in phenylalanine biosynthesis are oxidized via the respiratory chain, providing (P/O) moles of ATP for each mole of oxygen utilized. Analysis of the network in Figure 1 subject to these assumptions gives for Y_{ATP} the number of moles of ATP produced per mole glucose utilized:

for PTS uptake (case 1): $Y_{ATP} = 0.4 + 1.3\ (\text{P/O})$

for galactose symport uptake (case 1):

$$Y_{ATP} = -1.2 + 0.6\ (\text{P/O})$$

Assuming a (P/O) ratio of 2.0, the maximum theoretical yields of phenylalanine (mol of phenylalanine/mol of glucose) are

for PTS uptake (case 1): $Y_{PHE} = 0.275$

for galactose symport uptake (case 1):

$$Y_{PHE} = 0.55$$

These numbers are slightly different from previously reported theoretical yields (Forberg *et al.*, 1988; Forberg and Haggstrom, 1988) because of differences in the networks and assumptions considered. However, the qualitative conclusion, that switching from PTS to GalP uptake increases the theoretical yield of phenylalanine 2-fold, remains, and is also the same for the two cases considered here. Moreover, and extremely important relative to the studies reported next, the GalP strain has a major disadvantage in maximum theoretical energy yield.

Stoichiometric analysis such as that given above is useful to define the limiting cases if a given set of reactions occurs without any side or competing reactions. This is never the case in metabolism of a growing cell. Also, observed yields are determined by the *rates* at which competing processes occur. Since no suitable kinetic framework is available for the competing processes encountered in PTS- and non-PTS *E. coli* engineered to overproduce phenylalanine, experimental studies are necessary.

Experimental Studies. *E. coli* strains PPA305 and PPA316, each harboring the phenylalanine-overproduction plasmid pSY130-14, were used in this study. PPA305 carries a Tn10 transposon insertion mutation at *galP* (coding for galactose permease) which eliminates all residual glucose uptake activity by the galactose permease, GalP. This strain can transport glucose via the phosphotransferase (PTS) system. PPA316 lacks the PTS system and uses a proton−galactose symport system for glucose transport; glucokinase catalyzes subsequent ATP-dependent phosphorylation in this strain.

I. Phenylalanine Production. Initial experiments in comparing phenylalanine production between the engineered strains PPA305/pSY130-14 and PPA316/pSY130-14 were performed using shake-flask cultivations. Results are presented in Figure 2a,b. Arrows show the time when the temperature was shifted from 30 to 38.5 °C. Although PPA316/pSY130-14 grew to a

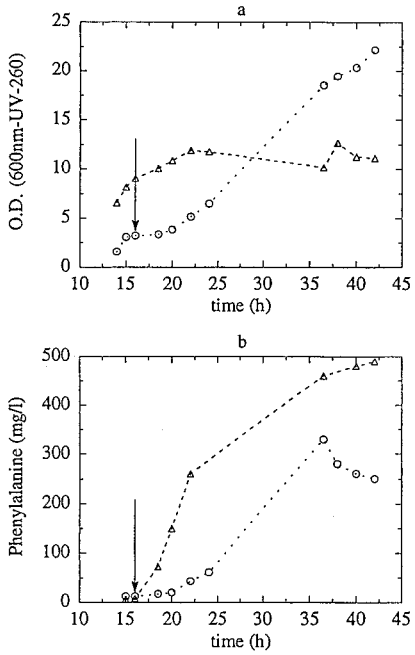

Figure 2. Time trajectories of biomass (a) and phenylalanine (b) during shaker-flask cultivation. Open circles: PPA316/pSY130-14. Open triangles: PPA305/pSY130-14.

much higher cell density than PPA305/pSY130-14 (70% higher in this case), the maximal phenylalanine concentration reached was considerably lower (330 versus 490 mg/L). Experiments using a uniform temperature of 38.5 °C gave qualitatively similar results, that is, the mutant grew to much higher cell density (90% higher) but produced much less phenylalanine (only one-fourth as much, 240 versus 960 mg/L).

Further investigation was done in a bioreactor. Figure 3a−c shows results from these cultivations. For the PTS strain PPA305/pSY130-14, phenylalanine production was growth-associated, reaching a highest phenylalanine concentration of 220 mg/L at the highest biomass concentration of 4.8 g/L. Afterward, when the medium glucose was depleted, phenylalanine was consumed quickly, and was depleted to one-tenth of its peak value within 3 h. PPA316/pSY130-14, in contrast to the PTS strain, did not produce any phenylalanine during the growth phase and produced 25 mg/L in stationary phase. PPA316/pSY130-14 reached a maximal biomass concentration of 4.4 g/L, slightly lower than the wild-type.

No byproduct (acetate, pyruvate, formate, lactate, or succinate) was detected in the supernatant for PPA316/pSY130-14. Only a trace amount of acetate accumulated in the growth medium of PPA305/pSY130-14. The maximal acetate concentration reached was only 0.1 g/L.

Samples taken from fermentor or shake flasks were properly diluted and spread on LB plates without kanamycin. After overnight cultivation, colonies on plates were counted. Colonies on replica plates (with kanamycin) were also counted. The plasmid stability as measured by this method was over 95% for both strains. There was no difference in stability between the two cultivation methods.

II. NMR Characterization. The same methodology as described elsewhere (Chen *et al.*, 1996) was applied here to further characterize the two strains PPA305/pSY130-14 and PPA316/pSY130-14. Assignments of the peaks and experimental procedures are detailed in Chen *et al.* (1996). Figure 4 shows typical spectra of whole cell suspensions, taken in quasi-steady-state glycolysis under aerobic conditions. The left part of the figure is the SP

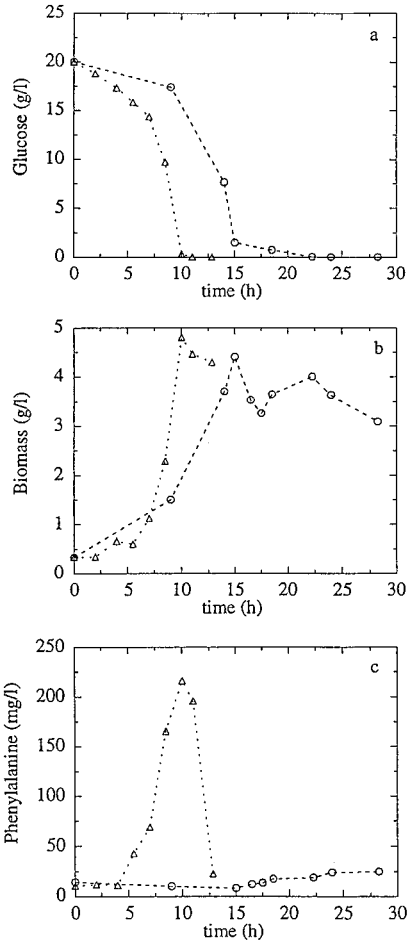

Figure 3. Time trajectories of glucose (a), biomass (b), and phenylalanine (c) during fermentations under aerobic conditions. Open circles: PPA316/pSY130-14. Open triangles: PPA305/pSY130-14.

and P_i region, and the right portion of the figure shows the vertically expanded nucleotide region (−4.5 to −20 ppm). Quantitative results are given in Table 1.

The absence of the P_i^{cyt} peak in the P_i region of the spectrum (Figure 4 bottom, left) for PPA316/pSY130-14 indicates a much lower ΔpH across the cytoplasmic membrane, relative to that in PPA305/pSY130-14. Although the sensitivity of the measurement does not allow estimation of an accurate value, the ΔpH was likely below 0.3 unit, since a pH difference of 0.3 units is likely the minimal value that allows differentiation of P_i peaks from two compartments (Campbell-Burk and Shulman, 1987). A substantially different energetic state of the strain PPA316/pSY130-14, compared to that of PPA305/pSY130-14, is also reflected by the 3-fold smaller pool of NTP. The NAD(H) concentration in the non PTS strain was 1.8 times lower than its PTS counterpart (Table 1).

The ratio of the total SP concentration in strain PPA316/pSY130-14, relative to that for strain PPA305/pSY130-14, was 2.4 based on the whole cell experiments. The compositions of the SP for both strains were determined by PCA extract NMR. Results are given in Table 2. As with PPA305 and PPA316 (Chen *et al.*, 1996), the most significant difference was found in fructose phosphate and PEP. PPA316/pSY130-14 had only one-sixth the PEP concentration and only one-seventh the fructose phosphate concentration of those of the PTS construct.

III. Analysis of Intracellular Fluxes. Mathematical analysis of the carbon flux distribution through the central carbon pathways has been successfully used to

Table 1. Intracellular Concentrations Measured by ^{31}P NMR on Whole Cell Samples[a]

	SP	NTP	NAD(H)	UDPG
PPA305/pSY130-14	36.1 ± 0.4	4.8 ± 0.2	9.0 ± 0.3	
PPA316/p130-14	15.2 ± 0.5	1.4 ± 0.2	5.1 ± 0.2	1.2 ± 0.3

[a] Concentrations are averages of at least three separate experiments.

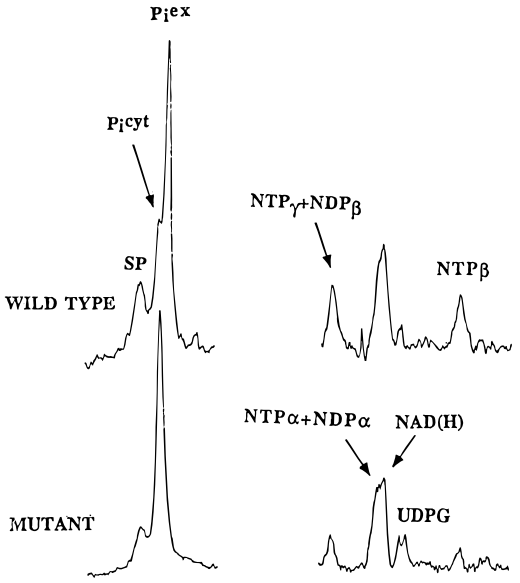

Figure 4. ^{31}P NMR spectra acquired during aerobic glycolysis of *E. coli* strains PPA305/pSY130-14 (top) and PPA316/pSY130-14 (bottom). The left part is for the SP and P_i region, and the right portion of the figure is vertically expanded nucleotide region. Spectra were obtained using 40° pulse and a relaxation delay of 0.2 s; NS (number of scans) 480; other parameters as in the Materials and Methods.

Table 2. SP Concentrations Measured by Extract ^{31}P NMR[a]

	PPA305/pSY130-14	PPA316/p130-14
G6P	1.0	2.2
3-PGA	0.6	1.3
FdP + F6P	28.6	4.2
2-PGA	5.5	2.1
SP-Un	1.4	3.3
SP total	37.1	13.1
PEP	18.6	3.1

[a] Concentrations are in mM and are averages of at least three separate experiments. SP-Un: unidentified sugar phosphate. Other abbreviations are the same as Figure 5. The relative error is equal to 20% (nd: not determined).

provide insight to the response of an organism to its environment and to characterize genetically engineered microorganisms (Reardon *et al.*, 1987; Vallino and Stephanopoulos, 1990; Goel *et al.*, 1993). To better understand the redirection of the carbon flux caused by the change of the glucose uptake system, we performed an intracellular flux analysis based on data from exponentially growing cultures.

The biochemical reaction network considered in our analysis (shown in Figure 5) includes the glycolytic (EMP) pathway, the pentose phosphate (PP) pathway, and the tricarboxylic acid (TCA) cycle. This is a simplified representation considering the fluxes to and from the precursor metabolites, as they are the main nodes in the network through which carbon flows to biomass and to product, as well as the fluxes that generate or consume energy and reducing equivalents.

Mass balance equations can be formulated for every metabolite in Figure 5, and by assuming a quasi-steady

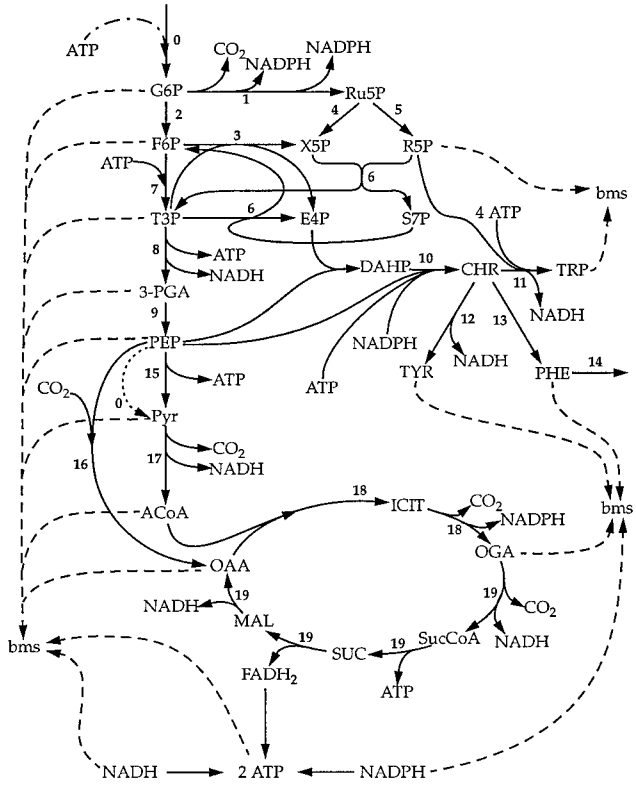

Figure 5. Biochemical reaction network considered in the analysis of the intracellular fluxes. The dotted arrow indicates the flux from PEP to pyruvate due to utilization of PEP for the glucose transfer from the PTS strain, in which case, the dotted-dashed arrow (flux from ATP) is not considered. Interchangeably, the flux depicted by the dotted-dashed arrow is considered for the non-PTS strain, for the ATP consumed for glucose transfer, and the flux depicted by the dotted arrow is not considered.

state, the following equation results:

$$\sum_j \alpha_{ij} V_j = 0 \qquad (3)$$

where α_{ij} is the stoichiometric coefficient of metabolite i in reaction j and V_j is the rate of reaction step j as numbered in Figure 5.

In our calculations, we used the growth data, the glucose consumption, and phenylalanine production data from 5 to 10 h and 8 to 15 h when the PTS and the non-PTS cells grow exponentially, respectively (Figure 3). Using these data we calculated the glucose uptake rate, the biomass production rate, the specific growth rate, the biomass yield, and the phenylalanine production rate: these results are presented in Table 3. The PTS strain grows 2.5 times faster than the non-PTS strain. However, the glucose uptake of the PTS strain is 1.4 times higher than that of the non-PTS strain.

In the analysis of the intracellular fluxes, we first considered that V_1 is the flux from G6P to Ru5P and, together with V_{18}, satisfies the theoretical NADPH biosynthesis requirement, as these are the NADPH-producing reactions in the central carbon pathways. The solution for this metabolic model predicted a flux from Ru5P to G6P which is not physiologically feasible and indicates that the NADPH production from TCA fulfills the biosynthetic requirements. In this case the enzymes that catalyze the processes represented by reaction step V_1 are repressed (Gottschalk, 1986). Therefore, we set V_1 equal to zero and we solved the system without considering the NADPH mass balance.

Table 3. Glucose Uptake Rate, Biomass Production Rate, Biomass Yield, Specific Growth Rate, and Phenylalanine Production Rate for the Two Strains[a]

	PTS	non-PTS	(non-PTS)/(PTS)
glucose uptake rate (mmol/h)	19.00	13.51	0.71
biomass production rate (g-dw/h)	0.92	0.47	0.51
growth yield coefficient, $Y_{x/s}$ (g-dw/mol of glucose)	48.42	34.79	0.72
specific growth rate, m (h^{-1})	0.20	0.08	0.40
phenylalanine production rate (mmol/h)	0.25	0.00	0.00

[a] Values were calculated by linear regression analysis of the data from 5−10 h and 8−15 h fermentations for the PTS and the non-PTS strains, respectively.

The number of mass balances in this metabolic scheme considered is equal to 18, and the number of unknown fluxes is also equal to 18 (17 fluxes are known). The set of the known fluxes includes the experimentally determined fluxes (such as glucose uptake rate (V_0) and phenylalanine production rate (V_{14})), and the fluxes to biomass synthesis which are estimated from the specific growth rate, μ, multiplied by the yields of precursors and reducing equivalents (NAD(P)H and FADH), as reported by Neidhardt *et al.* (1990).

The resultant flux distribution is presented in Table 4. The fluxes are normalized with respect to glucose uptake, indicating the moles of metabolites flowing through each step per mole of glucose consumed. The flux of carbon per mole of glucose through the glycolytic pathway appears to be the same for the two strains. However, the flux through the PP pathway is altered. This difference arises from the lower flux toward chorismate (CHR), V_{10}. This flux is probably limited by the low PEP concentration. Therefore, we tried to identify the possible reasons for the lower PEP levels.

The reactions from 3-PGA to PEP are considered to be in equilibrium (Gottschalk, 1986). P_i and H^+ influence these equilibrium steps. The lower ΔpH and P_i^{cyt} observed in the non-PTS strain indicate a shift in these equilibrium steps toward 3-PGA. This shift is confirmed by NMR data (Table 2). Therefore, in the non-PTS strain, the altered energetic status results in a triose phosphate pool with a lower PEP concentration. Moreover, the total concentration of the triose phosphate pool, as determined by NMR (Table 2), is much lower for the non-PTS strain, due to the differences in the fluxes from PEP to the TCA cycle.

The non-PTS strain has almost 3 times higher flux through pyruvate kinase (PYK; V_{15}). A higher flux through PYK is reasonable to produce ATP necessary in this strain for glucose uptake. This higher flux is channelled to the TCA cycle and results in an increased requirement for flux through PEP carboxylase. The higher flux through TCA leads to a 2.5 times higher production rate of reducing equivalents which are used by the cell to pump out the protons cotransferred with the glucose. Moreover, by assuming a respiration stoichiometry of two ATP/NAD(P)H and one $FADH_2$/ATP, we can calculate the maximum theoretical ATP yield for the two strains: 3.2 (g of dry weight)/(mol of ATP) and 1.9 (g of dry weight)/(mol of ATP) for the PTS and the non-PTS strain, respectively.

In general, a higher flux through an enzyme is normally associated with higher substrate concentration. The higher flux through PYK accordingly leads to the expectation of a higher PEP level in the non-PTS strain because it is one of the substrates of PYK. However, PYK is subject to allosteric regulation by FdP, which acts as an activator, ATP, which acts as an inhibitor, and ADP, which is the second substrate. Significant differences in the levels of these metabolites between the two strains imply the superposition of regulatory action in addition to substrate concentration effects on the flux through PYK. Therefore, we employed the reported kinetic expression for PYK in order to examine how the calculated ratio ($V_{PYK}/V_{PYK,max}$), evaluated at the measured concentrations of PEP, ATP, and FdP (Table 2), compares in the two strains.

Table 4. Calculated Intracellular Fluxes[a]

$(V_i/V_0) \times 100$	PTS	non-PTS	(non-PTS)/(PTS)
1	0	0	
2	99.0	99.3	1.00
3	3.48	1.88	0.54
4	3.91	2.50	0.64
5	3.91	2.50	0.64
6	0.43	0.62	1.44
7	94.8	96.5	1.02
8	185.	190.	1.03
9	178.	185.	1.04
10	3.05	1.25	0.41
11	0.26	0.19	1.72
12	0.63	0.46	0.72
13	2.15	0.61	0.28
15	58.	172.	2.98
16	13.9	10.0	0.72
17	144.	163.	1.13
18	126.	150.	1.19
19	121.	146.	1.21

[a] The numbers correspond to the reaction steps considered in Figure 5. For the experimentally determined fluxes used in the calculations, values were calculated by linear regression analysis of the data from 5−10 h and 8−15 h fermentations for the PTS and the non-PTS strains, respectively. The assumptions made for the calculation of the fluxes are discussed in the text (Analysis of Intracellular Fluxes).

We used the rate expression reported by Markus *et al.* (1980) and Boiteux *et al.* (1983) and presented in Table 5. We assumed the total Mg concentration, $[Mg_{total}]$, to be in the range 5−10 mM (Neidhardt *et al.*, 1990), the total adenylate concentration ([AN] = [ATP] + [ADP] + [AMP]) in the range 3−4 mM (Chapman *et al.*, 1971), and the adenylate kinase equilibrium constant (K_{eq} = ([ADP]^2/[ATP][AMP]) in the range 1−1.5. Within the range of the assumed values for the adjustable parameters, the ratio ($V_{PYK}/V_{PYK,max}$) calculated for the non-PTS strain was nearly twice as much as it was for the PTS strain. This difference indicates that the concentrations of the PYK regulators in the non-PTS strain double the activity of PYK. As a result, the flux through PYK is increased, even for a lower PEP level, draining PEP to the TCA cycle.

Discussion

In the course of fermentation of PPA316/pSY130-14, when cell density was over 3 g/L, aeration using fixed air flow rate (the same flow rate as used for the other strain) and maximal agitation speed (higher than that used for the other strain at higher biomass concentration) could not maintain the dissolved oxygen above 20% of air saturation. Oxygen enrichment was necessary in the later stage of the fermentation of this strain. Oxygen supply and utilization follows the following equation:

$$K_L a\{[O_2]^* - [O_2]\} = q_{O_2} X \qquad (4)$$

where $K_L a$ is the mass transfer coefficient, $[O_2]^*$ is the dissolved oxygen concentration in equilibrium with the gas phase, $[O_2]$ is the dissolved oxygen concentration, q_{O_2} is the specific oxygen uptake rate, and X is the biomass

Table 5. Pyruvate Kinase Rate Expression (Markus *et al.*, 1980; Boiteux *et al.*, 1983)

$$v_{PYK} = v_{m(PYK)} \frac{\alpha\beta\xi\phi G_1^{(n-1)}}{G_1^n + L_2 G_2^n + L_3 G_3^n}$$

where

$$G_1 = 1 + \alpha + \beta\xi\phi + \alpha\beta\xi\phi$$
$$G_2 = 1 + \beta + \alpha\beta\xi\phi$$
$$G_3 = 1 + \beta + \delta + \beta\delta$$
$$L_j = L_{jo}\frac{1}{(1+\varepsilon)^n}, \quad j = 2,3$$
$$\phi = \frac{1}{1 + c_1\alpha + (c_2 + \eta)\beta + (c_3 + c_4\eta)\delta}$$

$$\alpha = \frac{[PEP]}{K_{A_1}}, \quad \beta = \frac{[ADP]}{K_{B_1}}, \quad \delta = \frac{[ATP]}{K_{Q_3}}$$
$$\varepsilon = \frac{[FdP]}{K_{F_1}}, \quad \xi = \frac{[Mg_{total}]}{K_M}, \quad \eta = \frac{[H^+]}{K_H}$$

Parameter values :

K_{A_1} = 0.31 mM	K_{B_1} = 0.26 mM	K_{Q_3} = 22.5 mM
K_M = 2.077 mM	K_H = 0.055 mM	$[Mg_{total}]$ = 5–10 mM
K_{F_1} = 0.19 m M	c_1 = 0.056	c_2 = 0.333
c_3 = 225.0	c_4 = 390.0	$[H^+]$ = 10^{-6} – 10^{-8} mM
L_{2o} = 10^3	L_{3o} = 10^3	n = 4

concentration. The observed difference in dissolved oxygen (DO) profiles indicated a higher specific O_2 uptake rate in PPA316/pSY130-14. This strain produced lower final biomass concentration and no phenylalanine and no acetate, indicating that more carbon was oxidized to CO_2. Previous studies of control of the TCA cycle suggest that citrate synthesis plays a key role in regulating carbon flux to the TCA cycle, for which ATP, among other metabolites, is an inhibitor. The ATP level in this strain was unusually low as measured by NMR methods (Table 1, note: half of NTP is ATP; see Chen *et al.* (1996)). Therefore more carbon flux through the TCA cycle in this strain is likely responsible for the higher specific oxygen uptake rate and higher yield of CO_2. Mathematical analysis of the metabolic fluxes supports the above argument and suggests that this flux redistribution serves to increase production of reducing equivalents in the non-PTS strain to facilitate proton export and to improve the cellular energetic state.

Contrary to expectation, switching to a non-PTS system did not increase the PEP pool and did not enhance the production of phenylalanine. The reason for the low PEP level appears to be the increased flux through PYK which is mainly due to the regulatory characteristics of the enzyme. The levels of the regulators (FdP and ATP) and the second substrate (ADP) allow an increased PYK activity which can support a higher flux even for lower PEP levels. A conceivable strategy for higher PEP levels in the non-PTS strain is the replacement of the native PYK by one with lower affinity for FdP (no activation) which will be more sensitive to PEP. Such an approach could possibly result in intracellular PEP accumulation that could be channelled to phenylalanine production. Moreover, accumulation of PEP will result in higher levels for the triose phosphates and improved flux through the PP pathway.

Acknowledgment

The plasmid pSY130-14 was kindly provided by Dr. Toshiomi Yoshida (Osaka University, Japan). This work was supported by the National Science Foundation (Grant No. BCS 891284) and by the Swiss Priority Program in Biotechnology (SPP BioTech). The LH fermentor and instrumentation were generously provided by LH Fermentation (Hayward, CA). The assistance of Dr. Robert Lee with the Bruker AM500 NMR spectrometer is greatly appreciated.

Notation

3-PGA	3-phosphoglycerate
ACoA	acetyl coenzyme A
ADP	adenosine 5′-diphosphate
AMP	adenosine 5′-triphosphate
ATP	adenosine 5′-monophosphate
bms	biomass
CHR	chorismate
DAHP	3-deoxyarabinoheptulosonate 7-phosphate
E4P	erythrose 4-phosphate
F6P	fructose 6-phosphate
G6P	glucose 6-phosphate
Glc	extracellular glucose
Glu	glutamate
ICIT	isocitrate
NAD(H)	nicotinamide adenine dinucleotide (total)
NADH	nicotinamide adenine dinucleotide (reduced)
NADPH	nicotinamide adenine dinucleotide phosphate (reduced)
NDP	nucleoside diphosphate
NTP	nucleoside triphosphate
OAA	oxaloacetate
OGA	α-ketoglutarate
PEP	phosphoenolpyruvate
PHE	phenylalanine
P_i	inorganic phosphate
P_i^{cyt}	intracellular inorganic phosphate
P_i^{ex}	extracellular inorganic phosphate
Pyr	pyruvate
R5P	ribose 5-phosphate
Ru5P	ribulose 5-phosphate
S7P	sedoheptulose 7-phosphate
SP	sugar phosphate
TP	triose phosphate, or glyceraldehyde 3-phosphate
TRP	tryptophan
TYR	tyrosine
UDPG	uridinediphosphoglucose
V_i	flux through step *i* in Figure 5
X5P	xylulose 5-phosphate

Literature Cited

Backman, K.; O'Connor, M. J.; Maruya, A.; Rudd, E.; McKay, D. Genetic engineering of metabolic pathways applied to the production of phenylalanine. *Ann. N. Y. Acad. Sci. U.S.A.* **1990**, *589*, 16−24.

Bell, A. A.; Wheeler, M. H. Biosynthesis and Functions of Fungal Melanins. *Annu. Rev. Phytopathol.* **1986**, *24*, 411−451.

Boiteux, A.; Markus, M.; Plesser, T.; Hess, B.; Malcovati, M. Analysis of progress curves: Interaction of pyruvate kinase type from *Escherichia coli* with fructose 1,6-bisphosphate and calcium ions. *Biochem. J.* **1983**, *211*, 631−640.

Boos, W.; Ehman, U.; Bremer, E.; Midendorf, A.; Postma, P. W. Trehalase of *Escherichia coli*. Mapping and cloning of its structural gene and identification of the enzyme as a periplasmic protein induced under high osmolarity growth conditions. *J. Biol. Chem.* **1987**, *262*, 13212−13218.

Brown, K. D. Regulation of aromatic amino acid biosynthesis in *Escherichia coli* K-12. *Genetics* **1968**, *60*, 31−48.

Campbell-Burk, S. L.; Shulman, R. G. High resolution NMR studies of *Saccharomyces cerevisiae*. *Ann. Rev. Microbiol.* **1987**, *41*, 595−616.

Chapman, A. G.; Fall, L.; Atkinson, D. E. Adenylate energy charge in *Escherichia coli* during growth and starvation. *J. Bacteriol.* **1971**, *108*, 1072−1086.

Chen, R.; Bailey, J. E. Observations of aerobic, growing *Escherichia coli* metabolism using an on-line nuclear magnetic resonance spectroscopy system. *Biotechnol. Bioeng.* **1993**, *42*, 215−221.

Chen, R.; Bailey, J. E. Energetic effect of *Vitreoscilla* hemoglobin (VHb) expression in *Escherichia coli* : an on-line ^{31}P NMR and saturation transfer study. *Biotechnol. Prog.* **1994**, *10*, 360−364.

Chen, R.; Yap, W. M. G. J.; Postma, P. W.; Bailey, J. E. Comparative studies of *E.coli* strains using different glucose uptake systems: metabolism and energetics. *Biotechnol. Bioeng.* **1997**, in press.

Diaz-Ricci, J. C; Hitzmann, B.; Rinas, U.; Bailey, J. E.. Comparative studies of glucose catabolism by *Escherichia coli* grown in a complex medium under aerobic and anaerobic conditions. *Biotechnol. Prog.* **1990,** *6*, 326−332.

Draths, K. M.; Pompliano, D. L.; Conley, D. L.; Frost, J. W. ; Berry, A.; Disbrow, G. L.; Staversky, R. J.; Lievense, J. C. Biocatalytic synthesis of aromatics from D-glucose: the role of transketolase. *J. Am. Chem. Soc.* **1992**, *114*, 3956−3962.

Forberg, C.; Haggstrom, L. Phenylalanine production from a rec *Escherichia coli*-strain in fed-batch culture. *J. Biotechnol.* **1988**, *8*, 291−300.

Forberg, C.; Eliaeson, T.; Haggstrom, L. Correlation of theoretical and experimental yields of phenylalanine from non-growing cells of a rec *Escherichia coli* strain. *J. Biotechnol.* **1988**, *7*, 319−332.

Goel, A.; Ferrance, J.; Jeong, J.; Ataai, M. M. Analysis of metabolic fluxes in batch and continuous cultures of *Bacillus subtilis*. *Biotechnol. Bioeng.* **1993**, *42*, 686−696.

Gottschalk, G. *Bacterial metabolism*, 2nd ed.; Springer-Verlag: New York, 1986.

Hodgson, J. Bulk amino-acid fermentation: technology and commodity trading. *Bio/Technology* **1994**, *12*, 151−155.

Huang, S. O.; Gil, G. H.; Cho, Y. J. Kang, K. R.; Lee, J. H.; Bae, J. C. The fermentation process for L-phenylalanine production using an auxotrophic regulatory mutant of *Escherichia coli*. *Appl. Microbiol. Biotechnol.* **1985**, *22*, 108−113.

Konstantinov, K. B.; Nishio, N.; Seki, T.; Yoshida, T. Physiologically motivated strategies for control of the fed-batch cultivation of recombinant *Escherichia coli* for phenylalanine production. *J. Ferment. Bioeng.* **1991**, *71* (5), 350−355.

Markus, M.; Plesser, T.; Boiteux, A.; Hess, B.; Malcovati, M. Analysis of progress curves: Rate law of pyruvate kinase type I from *Escherichia coli*. *Biochem. J.* **1980**, *189*, 421−433.

Miller, J. E.; Backman, K. C.; O'Connor, M. J.; Hatch, R. T. Production of phenylalanine and organic acids by phosphoenolpyruvate carboxylase-deficient mutants of *Escherichia coli*. *J. Ind. Microbiol.* **1987**, *2*, 143−149.

Neidhardt, F. C.; Ingraham, J. L.; Schaecther, M. *Physiology of the bacterial cell: A molecular approach*; Sinauer Associates, Inc.: Sunderland, MA, 1990; Chapter 5.

Ogino T.; Garner, C.; Marley, J. L.; Hermann, K. M. Biosynthesis of aromatic compounds: ^{13}C NMR spectroscopy of whole *Escherichia coli* cells. *Proc. Natl. Acad. Sci. U.S.A.* **1982**, *79*, 5528−5832.

Patnaik, R.; Liao, J. C. Engineering of *Escherichia coli* central metabolism for aromatic metabolite production with near theoretical yield. *Appl. Environ. Microbiol.* **1994**, *60*, 3903−3908.

Pittard, A. J. Biosynthesis of the aromatic amino acids. In *Escherichia coli and Salmonella typhimurium cellular and molecular biology*; Neidhardt, F. C., Ed.; ASM: Washington, DC, 1987; Vol. I, pp 368−394.

Postma, P. W.; Lengeler, J. W.; Jacobson, G. R. Phosphoenolpyruvate phosphotransferase systems in bacteria. *Microbiol. Rev.* **1993**, *57*, 543−594

Reardon, K. F.; Scheper T. H.; Bailey, J. E. Metabolic pathway rates and culture fluorescence in batch fermentations of *Clostridium Acetobutylicum*. *Biotechnol. Prog.* **1987**, *3*, 153−167.

Sugimoto, S.; Yabuta, M.; Seki, T.; Yoshida, T.; Taguchi, H. Expression of pheA gene using P_R-P_L tandem promoter of bacteriophage lambda. *Appl. Microbiol. Biotechnol.* **1985**, *22*, 336−342.

Sugimoto, S.; Yabuta, M.; Kato, N.; Seki, T.; Yoshida, T.; Taguchi, H. Hyperproduction of phenylalanine by *Escherichia coli*: application of a temperature-controllable expression vector carrying the repressor-promotor system of bacteriophage lambda. *J. Biotechnol.* **1987**, *5*, 237−253.

Vallino, J. J.; Stephanopoulos, G. Flux determination in cellular bioreaction networks: applications to lysine fermentations. In *Frontiers in bioprocessing*; Sikdar, S. K., Bier, M., Todd, P., Eds.; CRC Press, Inc.: Boca Raton, FL, 1990; pp 205−219.

Weiss, U.; Edwards, J. M. *The biosynthesis of aromatic compounds*; Wiley: New York, 1980.

Zuraski, G.; Brown, K. D.; Killingly, D.; Yanofsky, C. Nucleotide sequencing of the leader region of the phenylalanine operon of *Escherichia coli*. *Proc. Natl. Acad. Sci. U.S.A.* **1978**, *75*, 4271−4275.

Accepted July 3, 1997.[⊗]

BP970060H

[⊗] Abstract published in *Advance ACS Abstracts*, September 1, 1997.